Energy Conversion and Management 87 (2014) 1027–1038

Contents lists available at ScienceDirect

Energy Conversion and Management

journal homepage: www.elsevier.com/locate/enconman

Pyrolysis of superfine pulverized coal. Part 1. Mechanisms of methane formation

Jiaxun Liu, Xiumin Jiang *, Jun Shen, Hai Zhang

School of Mechanical Engineering, Shanghai Jiao Tong University, Shanghai 200240, PR China

ARTICLE INFO

Article history:
Available online 7 August 2014

Keywords:
Superfine pulverized coal
Coal pyrolysis
CH_4 formation mechanism
Curve deconvolution
CO_2 gasification

ABSTRACT

The superfine pulverized coal has a greater potential for reducing NO_x emissions in the staged and oxy-fuel combustion technologies. The compositions and evolving processes of the volatile species during coal pyrolysis are important for understanding the pyrolysis mechanisms and pollution control strategies. In spite of numerous works focused on the description of coal thermal decomposition, the mechanism of formation reactions for particular gaseous products of coal pyrolysis like CH_4 remains unclear. In this paper, the mechanisms of CH_4 formation during superfine pulverized coal pyrolysis in N_2 and CO_2 atmospheres are investigated under non-isothermal conditions in a fixed-bed reactor. The effects of coal type, particle size and temperature on the evolved CH_4 and its formation mechanisms are analyzed. In addition, the total overlapped CH_4 evolution curves are resolved applying the deconvolution method through numerical analysis. Five constituent reaction complexes induced by different functional groups are recognized. Five CH_4 precursors involving in the CH_4 revolution during coal pyrolysis are confirmed, applying the solid-state ^{13}C NMR analysis. Different CH_4 formation mechanisms initiated from the thermal decomposition of the functionalities are concluded, with the products competing for the donatable hydrogen for stabilization.

1. Introduction

The thermal degradation of coal is a core technology in energy utilizations [1]. The pyrolysis process is an important initial step in coal combustion and gasification. The released volatiles control the ignition, the temperature, and the stability of the flame. The softening, swelling, agglomeration characteristics of coal particles are also related to the coal pyrolysis [2]. In addition, the pyrolysis reactions can provide basic information concerning thermal decomposition of individual functional groups and the coal molecular networks [3]. The overall species evolution released as volatiles and tars, accounts for up to 70% weight loss of the coal. The compositions of the species are important for understanding the pyrolysis mechanisms and pollution control strategies [4]. The evolving volatile products make remarkable changes in the surrounding environment, chemical structure, surface morphology and porosity of the coal particles [5]. More importantly, the released volatiles have notable effects on the precursors of the pollutants (such as NO_x, SO_2 and soot). The gaseous products evolved during coal pyrolysis, consist of aliphatic hydrocarbons (mainly CH_4), CO, CO_2, H_2, etc. The components significantly change the reaction environment. Especially, these reducing species such as CH_4, CO and nitrogen precursors can hinder the formation of NO_x under certain circumstances. Hence, the mechanisms of CH_4 formation are studied in this publication, with data on CO and nitrogen species to be discussed in a future work.

The proposal of combustion with superfine pulverized coal (i.e., the average particle size around or below 20 μm) has provided a new way to understand the effect of coal particle size on the combustion process [6]. Our previous research shows that the technique of superfine pulverized coal particle combustion has many advantages, such as better stability, higher combustion efficiency, lower NO_x and SO_2 emission, and better oxy fuel combustion performances than using conventional coal particles [5–10]. The preliminary study [8] shows that the coal with smaller particle sizes and higher volatile matter has a greater potential for reducing NO emissions in the staged combustion technology. This is because with the decrease of coal particle sizes, yield temperatures of the volatile matter move forward, and the amounts of pyrolysis gases such as CH_4, NH_3 and HCN increase significantly. The oxygen is insufficient under fuel-rich combustion conditions. The earlier the volatile matter is released, the more resident time there will be to reduce the formative NO. Additionally, the more pyrolysis

* Corresponding author. Tel.: +86 21 3420 5681.
E-mail address: xiuminjiang@sjtu.edu.cn (X. Jiang).

http://dx.doi.org/10.1016/j.enconman.2014.07.053
0196-8904/

gases are evolved, the easier it is to remove the existing NO in a reductive atmosphere. Therefore, the influence of coal particle sizes on the evolution of CH_4 is focused in this paper.

Coal has a complex structure with heterogeneous and variable constituents. The overall formation of a given product evolved from coal pyrolysis may consist of several chemical reactions [11]. The envelope profile of the particular product is composed of several superimposed peaks. These reactions overlap both regimes and temperatures, which derive from multiple sources. It is more useful to investigate coal pyrolysis under non-isothermal conditions, which can partly solve this overlapping problem. The inflection due to partial overlap of separate reactions is sensitive to the reaction rates, and may be amplified with the heating rates [12]. Thus, the properties of multiple peaks of different shapes may vary. Slow heating is helpful for separating the stages of pyrolysis [4]. Additionally, an accurate determination of coal particle temperature is possible at low heating rates. The chemical picture of coal molecular structure can be depicted as aromatic clusters linked by aliphatic bridges. The pyrolysis process is essentially the bond breaking and crosslinking reactions. The analysis of decomposition of functional groups related to the evolved products is useful to form a general picture of the coal pyrolysis process. This paper implements a numerical analysis method for the deconvolution of the multi-component evolving curves of the pyrolysis products. The resolved individual component lines are assigned to the different functional-group pools.

In spite of numerous works focused on the description of coal thermal decomposition, the mechanism of formation reactions for particular gaseous products of coal pyrolysis remains unclear. The mechanism of methane formation in coal pyrolysis has been the subject of some debate [13]. Arenillas et al. [14] studied coal pyrolysis behavior using simultaneous thermogravimetry-mass spectrometry, and pointed out that the lower rank coals with more functional groups produced higher emission of CH_4. Porada [11] claimed that during coal pyrolysis, methane was formed as a result of six constituent reactions. Arenillas et al. [15] suggested that methane was formed in three different steps. Different methane evolution temperature ranges were the results of the breakage of aryl–alkyl-ether bonds, cleavage of methyl groups and secondary devolatilization. Cramer [16] displayed the isotope trend of methane from coal pyrolysis, and methane evolution might be interpreted as the result of the mixing of three individual reaction complexes. Jüntgen and van Heek [17] placed emphasis on the kinetics of gas formation, and pointed out the formation of methane involved two to four parallel and overlapped reactions [18]. Kelemen and Kwiatek [19] pointed out that the thermolysis of labile chemical bonds would initiate a complex series of reactions, leading to the evolution of light gases. Hodek et al. [20] investigated the reactions of oxygen containing structures during coal pyrolysis, and realized the main volatilization was attributed to the bond cleavage of alkyl–aryl-ethers. The formation of methane at higher temperatures was induced by the rearrangements of the primarily formed radicals.

There are few reports concerning the particle size effect on the pyrolysis mechanism, not to mention the systematic studies about the pyrolysis process of the superfine pulverized coal. In this paper, pyrolysis experiments of superfine pulverized coal were carried out under non-isothermal conditions, applying the fixed-bed reactor. The effects of coal type, particle size and temperature on the evolved methane and the formation mechanism were analyzed. The deconvolution of the overall methane evolving curves was conducted through numerical analysis. The individual component lines induced by the different functional-group pools are studied thoroughly, combining ^{13}C solid-state nuclear magnetic resonance (NMR) analysis.

2. Experimental section

2.1. Materials

Two typical Chinese coals from different geographic locations, Shenhua (SH) and Neimongol (NMG), were chosen for this study. The properties of the coals are listed in Table 1, from which it can be inferred that both SH and NMG coal samples are medium volatile bituminous coals with obvious differences in the extent of coalification. Coal samples were pulverized into small particles, with the sizes between 10 μm and 55 μm. The specific equivalent mean particle sizes of SH samples are 14.7, 17.4, 21.3 and 44.2 μm, while NMG samples are 12.5, 14.9, 25.8 and 52.7 μm. The particle sizes are so small that the effect of temperature distribution within the sample particle is eliminated [21]. During the process, the samples were not sieved to guarantee that the experimental data is in good agreement with the whole coal properties.

2.2. Apparatus and procedure

The coal pyrolysis experiments were carried out in a fixed-bed reactor, which is depicted in Fig. 1. The coal samples were heated in the quartz pipe furnace by a programmed temperature controller in high-purity N_2 (>99.999%) or CO_2 (>99.999%) atmospheres. The electrically heated part is 1000 mm long in the furnace, where the highest wall temperature can reach 1000 °C with a maximum heating rate of 35 °C/min. The flow rate of the carrier gas was heated before entering the bed, which was regulated to 3 L/min by a mass flow controller. About 0.4 g dry coal samples were placed in a porcelain boat, and heated up to 400, 600, and 800 °C at a constant heating rate. The compositions of outlet gases at the exit of the furnace were analyzed by a portable FTIR (Fourier transform infrared) gas analyzer Gasmet DX-4000 (Finland), which is an on-line real-time detecting system. The detailed description can be found elsewhere [8]. In our case, the evolving products during coal pyrolysis, including CH_4, CO, NH_3, NO, N_2O, NO_2, HCN, CO_2, SO_2, H_2O, HCl and HF, can be measured quantitatively by Gasmet. The lowest detectable concentrations are 0.1–2 ppm, and the accuracy is 2%, depending on the application.

2.3. Solid-state ^{13}C CP/MAS/TOSS NMR analysis method

The solid-state ^{13}C nuclear magnetic resonance (NMR) spectroscopy has been widely applied to directly characterize the carbon structural features and functional groups in fossil fuels. All the high-resolution ^{13}C NMR experiments were performed on a Bruker Advance 400 MHz NMR spectrometer (Germany), operating at a ^{13}C frequency of 100.63 MHz. The cross polarization (CP) and magic

Table 1
Ultimate and proximate analysis of tested coal samples.

Proximate analysis (mass %) (ad)		Ultimate analysis (mass %) (ad)	
SH			
Moisture	11.5	C	63.13
Volatile	24.22	H	3.62
Ash	10.7	O	9.94
Fixed carbon	53.58	N	0.70
		S	0.41
NMG			
Moisture	14.72	C	54.82
Volatile	35.69	H	4.39
Ash	10.64	O	14.58
Fixed carbon	38.95	N	0.63
		S	0.22

ad – on an air dried basis.
O content is calculated by difference.

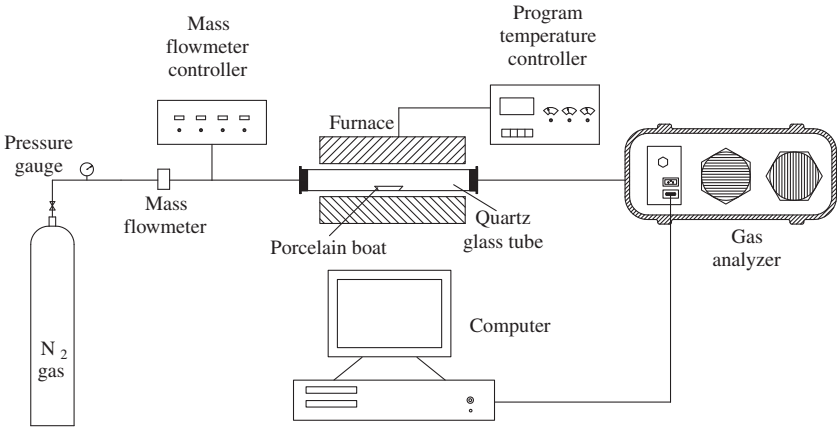

Fig. 1. Sketch map of the fixed bed reactor experimental system.

angle spinning (MAS) techniques were applied to improve signal-to-noise ratios for solid hydrocarbons. In addition, the total sideband suppression (TOSS) technique was employed to remove the sidebands. Coal samples were packed into a 4 mm diameter zirconia rotor and spun at 5 kHz. CP/MAS experiments were performed at a ^{13}C–^{1}H CP contact time of 1 ms and a pulse repetition delay of 4 s.

2.4. Thermogravimetric analysis (TGA) method

Thermogravimetric analysis (TGA) pyrolysis experiments are extensively applied to characterize thermal behaviors and pyrolysis kinetics of coals. The relationships between the weight loss and corresponding temperatures are recorded. All the TGA pyrolysis experiments in this work were carried out on the Q600 simultaneous DSC-TGA (America). About 10 mg coal samples were heated from ambient temperature to 1000 °C at a heating rate of 20 °C/min. A constant flow of 100 mL/min high-purity N_2 was blown into the furnace to ensure an inert atmosphere during the pyrolysis process. The precision of the apparatus can reach 0.1 μg of the weigh loss and 0.01 °C of the temperature.

3. Results and discussion

3.1. Influences of coal rank and particle size on the CH_4 formation mechanisms

The evolution profiles of CH_4 during SH and NMG coal pyrolysis in the N_2 atmosphere are shown in Fig. 2. The fixed-bed reactor was heated from room temperature up to 800 °C at stable heating rates of 20 °C/min. The CH_4 formation curve shows a single peak, extending over a wide temperature range from around 200 °C to about 800 °C, which is attributed to the multi-component structure with several superimposed peaks [18]. The major proportion is generated within 400–600 °C, with the main peak occurring at around 500 °C. Furthermore, all the methane evolution curves of SH coals are higher than those of NMG coals, i.e., higher-ranking coals release more methane during pyrolysis process. The loss of oxygen functionalities during maturation may increase the concentration of the CH_4 precursors.

Fig. 3 reveals the influence of coal rank and particle size on the maximum evolution temperatures of CH_4 under the same pyrolysis conditions (N_2 atmosphere, heating rates 20 °C/min.). The evolution rates and overall peak temperatures change for different ranking coals. Basically, all the maximum evolution temperatures of SH coals are higher than that of NMG coals, i.e., the peak temperatures shift towards higher temperatures with the increase of coal ranks. This is related to the macromolecular structures of coal. During coalification, functional groups with weaker bonds have been preferentially eliminated. The NMG coals with lower coalification extent have larger proportions of aliphatic side chains and bridges. During pyrolysis, thermal cleavages are prone to happen between these relatively weak bridges and linkages with lower bond dissociation energy once the decomposition begins. Thus, more fragments and functional groups like $-CH_3-$, $-CH_2-$, $-(CH_2)_2-$, $-(CH_2)_3-$, and $-C_2H_5$ are produced in lower ranking coals. These radicals can be stabilized by the donatable hydrogen to further release gaseous CH_4. Thus, more active groups and radicals are

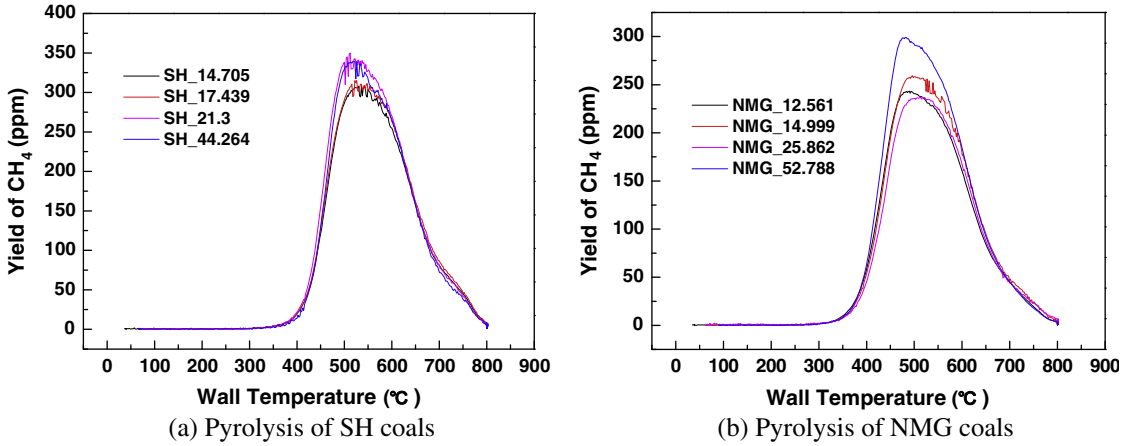

Fig. 2. Evolution of CH_4 during coal pyrolysis in the N_2 atmosphere (heating rates 20 °C/min, temperature 800 °C, N_2 atmosphere).

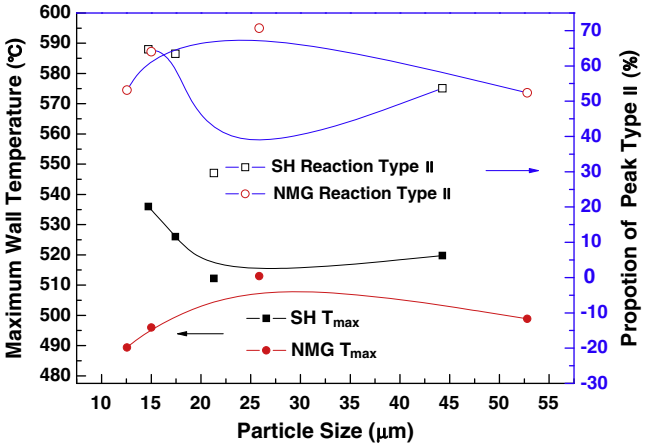

Fig. 3. Wall temperature of the maximum evolution rate of CH_4 (heating rates 20 °C/min, temperature 800 °C, N_2 atmosphere).

available, and the instantaneous formation rate of CH_4 inside the particle increases in lower ranking coals. Therefore, the peak temperatures are lower for NMG coals.

With the decrease of particle size, the specific surface area increases significantly, and more active sites are available. The heat and mass transfer effects in coal are enhanced. Therefore, the instantaneous formation rate of CH_4 inside the particle increases, and the escaping energy barrier decreases. Both can promote the release of CH_4 in smaller coal particles. However, there is a critical particle size for the maximum evolution of CH_4. When the particle size decreases to a certain extent, the resident time of the instantaneously evolved hydrocarbon fragments in the particles is shortened. Most of these fragments are released before the secondary pyrolysis reactions even happen. The heat and mass transfer resistance increases, and the amounts of the evolved CH_4 are reduced. Decreasing particle sizes can reduce the holdup of volatiles within the particle, which is an important source for methane evolution. Furthermore, with further decreasing of particle sizes, micropore structures increase evidently, and the adsorption effects are enhanced. Thus, the release of CH_4 will be retarded, and the maximum evolution temperatures will be delayed. We can observe from Fig. 3 that the evolution rate of CH_4 is largest for SH_21.3 coal samples, while NMG coals with particle sizes of 12.5 μm have the lowest peak temperatures. The larger quantities of CH_4 are produced, and the faster they are released, the more resident time there will be to reduce the existing NO_x. Therefore, the conclusion can be drawn that the lower ranking coals with relatively small particle sizes have stronger reduction effects of light hydrocarbons.

The influence of particle size on the mass loss during coal pyrolysis (N_2 atmosphere, heating rates 20 °C/min.) was further investigated through TGA analysis, shown in Fig. 4. The same trends of the TG and DTG curves can be observed among different particle sizes, which suggest the similar pyrolysis behaviors of the chemical bonds, and the influence of internal heat/mass transfer on pyrolysis is small. However, the deviations among the curves indicate the effect of particle sizes on the volatile releasing process. The three separated peaks of DTG curves divide the pyrolysis process into three main stages. The elimination of moisture in the coal samples occurs before 140 °C. The lower temperature stage between 350 and 600 °C coincides with the main releasing range of CH_4 that contributes a lot to the weight loss of this stage. Other contents of light hydrocarbon released during this range such as C_2H_4 (about 20 ppm) and C_3H_8 (about 50 ppm) are small (see Fig. 5). There is also a small peak around 700 °C, which is due to the cleavage of oxygen-containing structures with high bonding energies.

It can be observed from Fig. 4 that the mass loss rate of DTG curve shifts towards lower ranges, and the initiating temperatures of volatile matter decrease for smaller coal samples. This is in agreement with the results from Fig. 3 that the maximum evolution temperatures are lower for superfine pulverized coal. On the other hand, the maximum mass loss rate of DTG curve shows an increasing trend for larger coal particles, which can be seen more clearly from the magnified pictures in the figure. This is because the release of volatile matter becomes more promptly and intensely for smaller coal particles. Therefore, the initial concentrations and partial pressure of CH_4 around coal surfaces are higher for smaller coal. The diffuse of CH_4 from the interior of the particles into the gas space is retarded and the further release of CH_4 is hindered. Furthermore, the content of methane precursors in parent coal is also important for the yields of CH_4, which will be further analyzed in Section 3.2.

The heterogeneity and variability of coal indicate the complex character of its pyrolysis behaviors. The released products are formed from several different structural components. The decomposition of individual assumed functional groups in the coal and char can produce gas species. The evolution contains several different reaction sequences, which is a parallel process that competes for all the functional groups in the coal [4]. The roles of individual groups in different chemical processes are not yet well known in research. In this paper, the deconvolution method through numerical analysis was adopted to resolve the overall evolving curves of CH_4, applying computer techniques. After deconvolution of the overlapped releasing curves, individual component lines could be numerically analyzed. The properties of different types of functional groups contributing to the individual component lines were further investigated.

The distinctive temperature ranges of the degradation of heterogeneous complexes in various stages overlap each other, which causes the wide formation curves of methane. Previous studies show that methane was formed as a result of two to six constituent reactions [11,13,16]. Therefore, the CH_4 generation trends were simulated by introducing two to six independent Gaussian reaction complexes by varying the peak parameters like the locations, linewidths, and intensities. The approximations of the experimental curves by the superposition of five Gaussian lines, which gave the highest correlation coefficients (i.e., the smallest values of the root mean square deviation), were considered as the best fitting curves. The multi-component structures of CH_4 evolution rates of SH_14.7 and NMG_14.9 coals in the N_2 atmosphere are studied applying numerical analysis methods, shown in Fig. 6 (the similar results of other particle sizes are not shown here). The correlation coefficients of the lines are all greater than 0.999, which make the validity of the simulation preferable.

Three main reaction stages of CH_4 evolution during coal pyrolysis are clearly visible in Fig. 6. The stage one can be recognized in the range between 300 and 550 °C, where the revolution of CH_4 begins around 300 °C, followed by a steep increase trend and reaches the maximum at about 500 °C. The stage one can be simulated by two parallel reactions, peak I and peak II. The reaction type I is related to the methoxy groups in coal. The bonds between carbon and hetero atoms such as sulphur and oxygen are weaker, which are prone to be broken at lower temperatures. The demethylation of methoxyl groups is considered as an important source for the methane released at lower temperatures during coal pyrolysis. The mechanism of the methane evolution from the primary pyrolysis of methoxyl groups is shown in Eq. (1). Van Heek and Hodek [22] draw the similar conclusions that methane evolution within the lowest temperature range was a result of cleavage of aryl–methyl-ether bonds.

$$(\text{coal})\text{Ar}-\text{O}-\text{CH}_3 \rightarrow (\text{coal})\text{Ar}-\text{O}\cdot + \text{CH}_3\cdot \xrightarrow{\text{H}\cdot} \text{CH}_4 \quad (1)$$

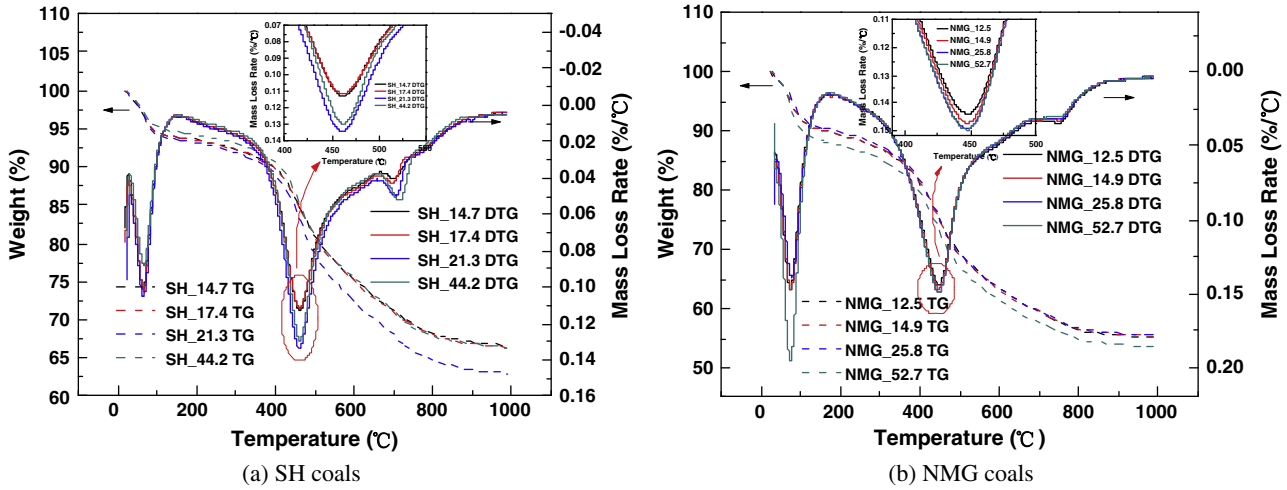

(a) SH coals (b) NMG coals

Fig. 4. TG/DTG curves of coal samples with different particle sizes (heating rates 20 °C/min, temperature 1000 °C, N_2 atmosphere).

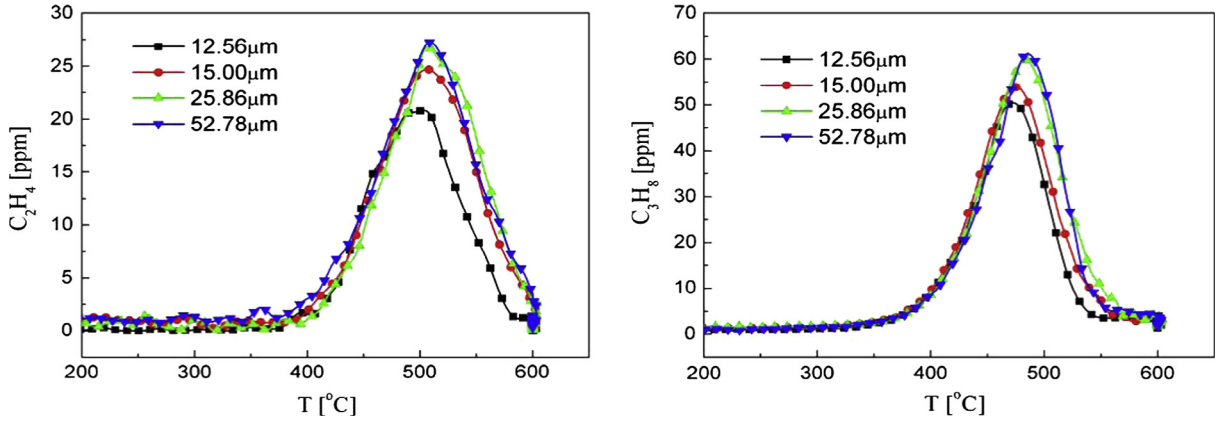

(a) C_2H_4 (b) C_3H_8

Fig. 5. Effect of particle size on evolution profile of light hydrocarbon (NMG coals, heating rates 20 °C/min, temperature 600 °C, N_2 atmosphere).

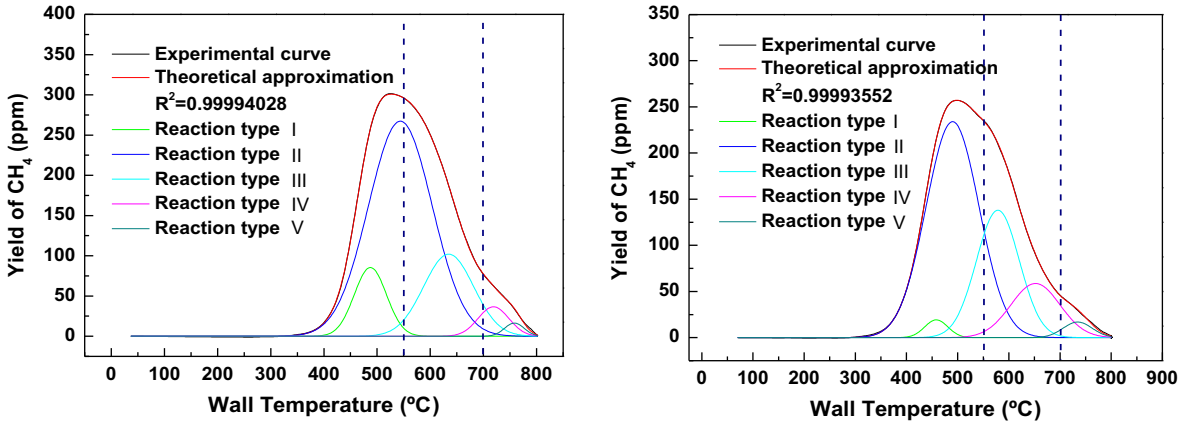

(a) Pyrolysis of SH_14.7 coals (b) Pyrolysis of NMG_14.9 coals

Fig. 6. Multi-component structure of CH_4 evolution rates during pyrolysis in the N_2 atmosphere (heating rates 20 °C/min, temperature 800 °C, N_2 atmosphere).

The reaction type II is also responsible for the low-temperature CH_4, which contributes to the major source of methane generation. The cleavage of long aliphatic chains, e.g. alkyl side chains, results in the evolution of this type of methane and its homologues [22,23]. Eq. (2) reflects the mechanism of the reaction-type- II methane evolution. The reaction type II is related to the release of β-methyl groups, which has lower bonding energies than aryl methyls (methyls on aromatic rings, i.e., α-methyl groups). Then, small aliphatic gas molecules especially CH_4 are generated through the rapid recombining reactions between these small radicals by

dissociation of the long aliphatic chains and hydrogen donors. This process explains the simultaneous occurrence of ethane and propane generation in the similar temperature range (300–500 °C) [24].

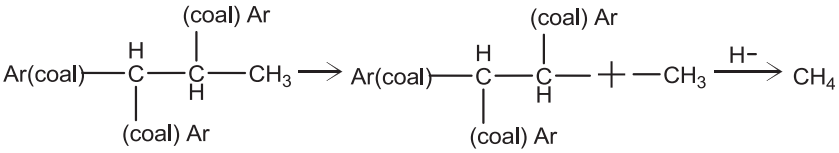

(2)

The NMR analysis was applied to testify the validity of alkyl decomposition mechanism of methane. NMR spectra were also interpreted by using a curve resolution method. All the total curves could be best fitted by around 20 mixed Gaussian–Lorentzian lines according to the chemical shifts of different functionalities in coal, which had distinctive lineshapes, linewidths, and intensities. Multicomponent structures of NMR spectra of SH and NMG coals are reflected in Figs. 7 and 8. Three parameters of ^{13}C NMR analysis are involved here, f_a^s, f_{am}, and f_{al}^H, which represent the alkyl-substituted aromatic carbons, aryl methyl carbons, and methylene carbons, separately. Chemical shift values [25] of alkyl-substituted aromatic carbons (f_a^s) lie in the range of 135–150 ppm, while aryl methyl carbons (f_{am}) are between 16 and 22 ppm. The methylene and methine groups in rings and chains are taken for chemical shift values of 22–50 ppm. All the parameters are obtained by calculating the ratio of integrating the spectral regions of each functional group to the integration of the total signal intensity. Table 2 compares the evolution of methane with the concentration of alkyl-substituted aromatic carbons in SH coals. It illustrates that the proportions of reaction peak II are positively correlated to the concentrations of alkyl functionalities, which cross link aromatic and naphthenic structures. Furthermore, it is interesting to note from Fig. 3 that the reaction complex II significantly influences the overall maximum CH_4 evolution temperatures. The larger the proportions of constituent reaction II are, the higher the overall maximum CH_4 evolution temperatures are.

The stage two is assigned to the temperature range of 550–700 °C, where the revolution of CH_4 begins to decline, which also

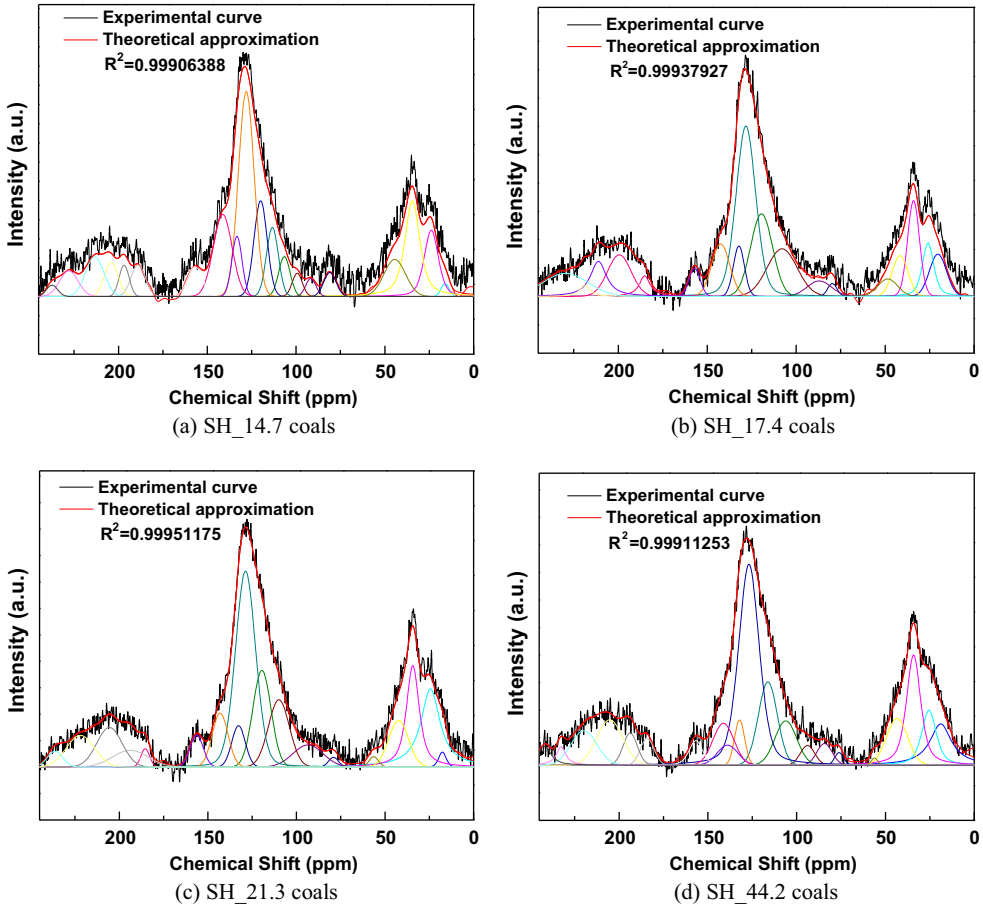

Fig. 7. Multi-component structures of NMR spectra of SH coal samples (raw coals).

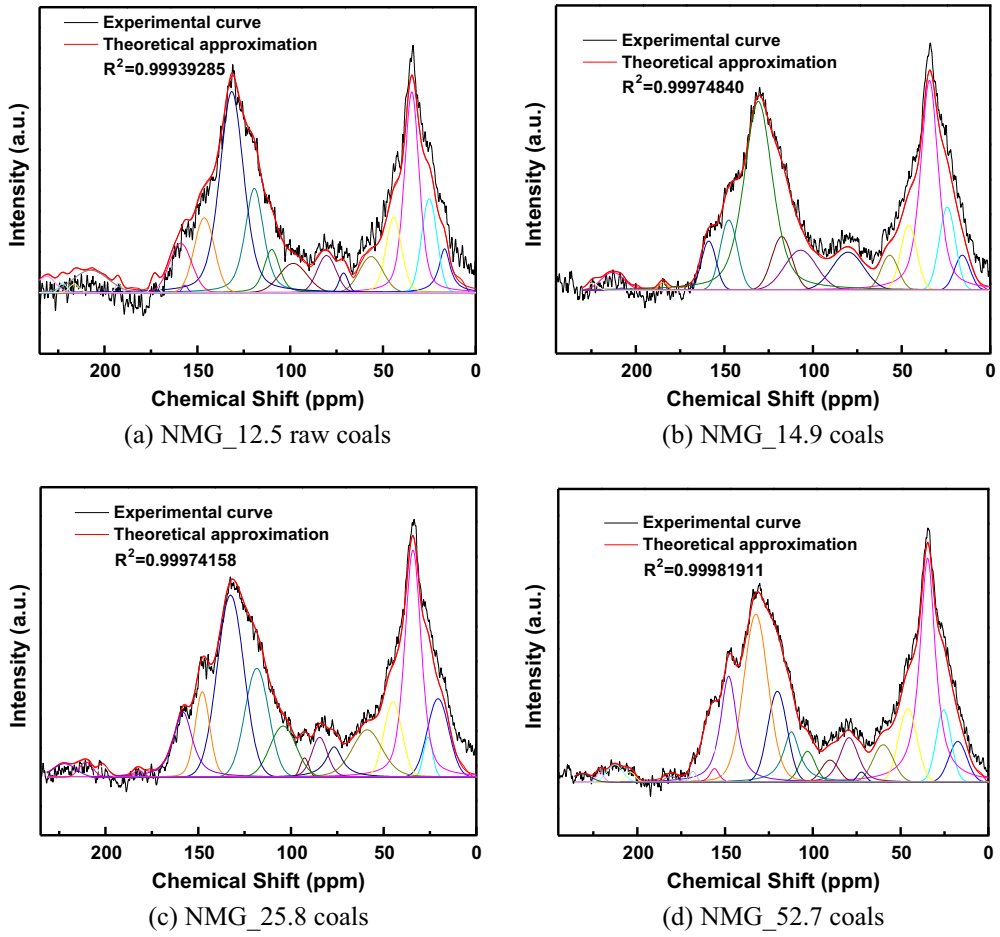

Fig. 8. Multi-component structures of NMR spectra of NMG coal samples (raw coals).

Table 2
Relationships between CH_4 reaction type and coal structures from NMR analysis (heating rates 20 °C/min, temperature 800 °C, N_2 atmosphere).

Samples	Alkyl-substituted aromatic carbons (%)	Reaction type II (%)	Aryl methyl carbons (%)	Reaction type III (%)	Methylene/methine carbons (%)	Reaction type IV (%)
SH_14.7	9.00	64.71	8.52	19.35	19.24	4.27
SH_17.4	5.35	63.47	8.50	16.54	13.99	10.15
SH_21.3	4.79	29.61	12.48	30.95	23.20	27.77
SH_44.2	5.31	53.64	11.42	28.29	17.46	5.51

contains two reaction complexes, peak III and peak IV. The relationships between aryl methyl groups and reaction type III CH_4 evolution are also displayed in Table 2. The reaction type III is positively related to the concentrations of aryl methyl groups, which are recognized as the methane precursors of peak III. The methyl groups located on aromatic rings with higher bonding energies are strongly fixed to coal macromolecules, and are eliminated only above 500–600 °C [26–28]. The methyl groups are splitting off from aromatic rings, with the formation of methyl units and radicals containing benzene structures. Then, the rapid recombining reactions among the small radicals (especially donatable hydrogen) take place, with the evolution of CH_4 and benzene. This explains the phenomena that methane and benzene appear at the same time in high amounts in this temperature range (around 550 °C) [20]. Eq. (3) reviews the methane-evolution mechanism of the reaction type III.

$$(\text{coal})\text{Ar}-\text{CH}_3 \rightarrow (\text{coal})\text{Ar}\cdot + \text{CH}_3\cdot \xrightarrow{\text{H.}} \text{CH}_4 \quad (3)$$

Table 2 provides the information that the methane evolution of the reaction type IV is related to the quantities of methylene and methine groups in coal. The secondary pyrolysis reactions of C_{2+}-hydrocarbons are one possible source for this type of methane [16]. The onset of tar formation at lower temperatures (around 350 °C) is the distillation and diffusion of organic molecules. The pore openings in the three-dimensional cross-linked molecular network of coal are so small (less than 5 Å) that larger molecules are believed to be trapped in the narrow pore structures. The polynuclear systems with higher molecular weights cannot diffuse fast enough within the coal particle, and are susceptible to be decomposed at higher temperatures. The secondary cracking reactions are initiated when the temperature reaches above 550 °C, with additional methane to be released. The secondary pyrolysis mechanism of methane evolution is shown in Eq. (4). Additionally, the reaction type IV, which is produced through secondary pyrolysis reactions, is also an important source of methane.

$$(\text{alkyl, aryl, H, etc.})\text{R}-\text{CH}_2-\text{CH}_3 \rightarrow \text{RCH}_2\cdot + \text{CH}_3\cdot \xrightarrow{\text{H.}} \text{CH}_4 \quad (4)$$

The stage three is responsible for the formation of methane after 700 °C, where only one constituent reaction V is observed. The cleavage of aromatic heterocyclic structures might be responsible for the release of this late methane [11,22,27]. These structures split off methane only at high temperatures (>700 °C) [19]. Only small amounts of CH_4 are yielded during this stage, which means the reaction complex V is not the main reaction type for methane evolution during coal pyrolysis.

In addition, the carbon–dihydrogen reaction can also induce the methane evolution at high temperatures, especially in hydropyrolysis process of coal in the presence of excess dihydrogen. This reaction can be remarkably enhanced by the hydrogen pressure. The mechanism is described in Eq. (5), which does not exist in our experiments.

$$C(\text{solid}) + 2H_2 \rightarrow CH_4 \quad (5)$$

3.2. Influence of pyrolysis atmosphere on the CH_4 formation mechanisms

With serious global warming and climate changing problems emerging, CO_2 emissions from coal combustion have drawn more attention. The O_2/CO_2 combustion method is recognized as a highly cost-effective and promising clean combustion technology on CO_2 control [29]. As mentioned in our previous work [8] that the combination of O_2/CO_2 combustion and superfine pulverized coal combustion technology can make full use of their respective merits and solve certain inherent disadvantages of each technology. However, CO_2 affects the coal pyrolysis significantly because CO_2 is a product and a reactant during coal degradation. Therefore, pyrolysis studies in the CO_2 atmosphere need to be accomplished for better understanding of the combustion and pollutants emission characteristics of oxy-fuel combustion [30].

Fig. 9 reflects the evolution profiles of CH_4 during SH and NMG coal pyrolysis in the CO_2 atmosphere. The temperatures were raised from the ambient temperature up to 800 °C at stable heating rates of 20 °C/min. The CH_4 formation curve shows a similarly wide spread single peak as in the N_2 atmosphere. The influence of atmospheres on the total yields of CH_4 is calculated and displayed in Fig. 10. The total yields of methane during pyrolysis in the CO_2 atmosphere are all basically lower than those generated in the N_2 atmosphere. This is because the density and heat capacity of CO_2 are significantly higher than those for N_2 [31]. The thermal diffusivity of CO_2 is lower, but the gas emissivity is higher. Thus, more heat is absorbed by the surrounding environment, and the energy exerted on the coal particles is reduced. The bond cleavage reactions are depressed, which leads to the decrease of the methane precursors and the subsequent methane evolution. In addition, the mass diffusivity of CH_4 in the CO_2 atmosphere is 20% lower than in N_2 [32], so that the diffuse of CH_4 from the interior of the particles into the gas space is retarded. The higher partial pressure of methane around the particle surfaces is expected to hinder the formation of CH_4. Therefore, the initial CH_4 concentrations and partial pressure increase in the CO_2 atmosphere. The reducing atmosphere exists longer around the particle surfaces, which provides advantages in eliminating NO_x. It is the same reason that promptly released methane from smaller coal particles will depress its total productivity. So the increasing trend of total methane yields is observed with the increase of coal particle sizes. This is supported by the observation from the TGA experiment in Fig. 4. Furthermore, we also summarized the proportions of all the possible precursor sources of CH_4 (i.e., the sum of the contents of alkyl-substituted aromatic carbons, aryl methyl carbons and methylene/methane carbons in coal) in the figure. It is interesting to notice that the total yields of CH_4 during coal pyrolysis are closely related to the precursor sources in parent coal.

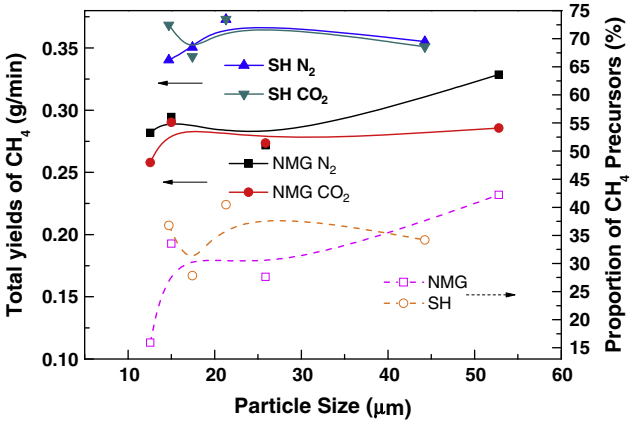

Fig. 10. Influence of atmospheres on the total yields of CH_4 (heating rates 20 °C/min, temperature 800 °C, N_2 and CO_2 atmosphere).

The influence of atmospheres on the reaction types of CH_4 can be concluded from the lineshapes of evolution curves, which is shown in Fig. 11. It can be observed that the peak widths of methane evolution in the CO_2 atmosphere are all narrower than those in the N_2 atmosphere. This means either there are less reaction types or the constituent reaction complexes are more overlapped during

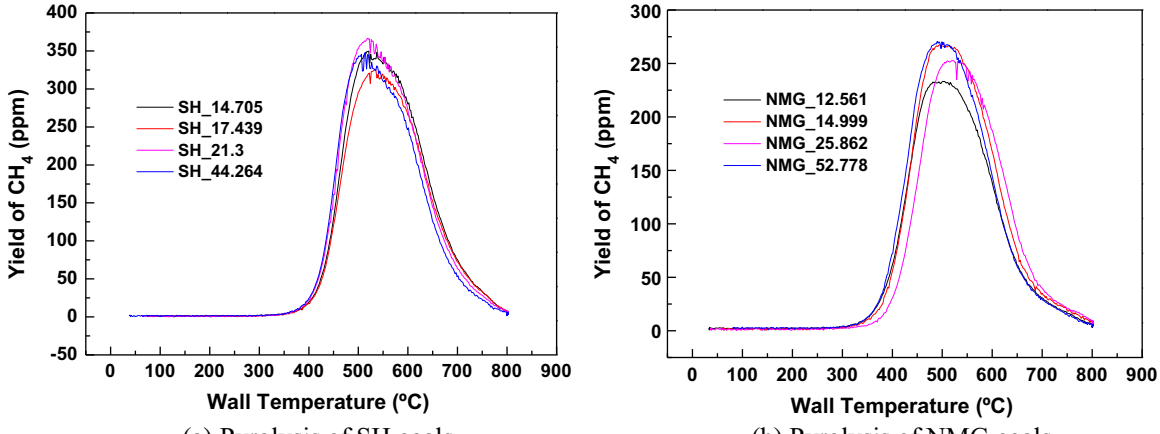

(a) Pyrolysis of SH coals (b) Pyrolysis of NMG coals

Fig. 9. Evolution of CH_4 during coal pyrolysis in the CO_2 atmosphere (heating rates 20 °C/min, temperature 800 °C, CO_2 atmosphere).

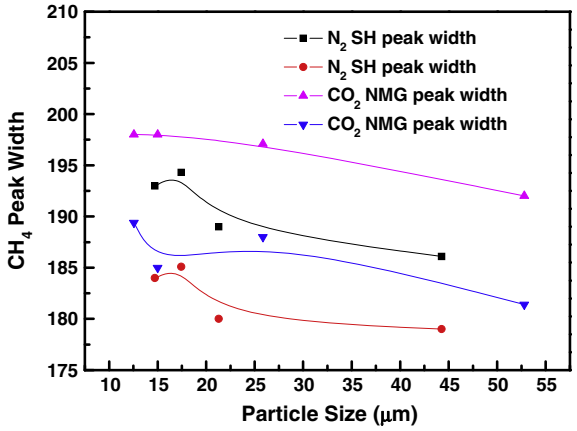

Fig. 11. Influence of atmospheres on the overall lineshapes of CH_4 evolution curves (heating rates 20 °C/min, temperature 800 °C, N_2 and CO_2 atmosphere).

coal pyrolysis in the CO_2 atmosphere, which will be illustrated in the following curve resolving analysis.

Replacing N_2 with CO_2 seems to enhance the CH_4 releasing rate, and the maximum evolution temperatures shift towards lower temperatures. This is related to the constituent reactions, which can be analyzed through the deconvolution methods. The overall CH_4 evolution curves from the CO_2 atmosphere can also be best fitted by five Gaussian lines. Therefore, pyrolysis atmospheres have no measurable effects on the numbers of the constituent reactions leading to the bulk generation curve of methane. The multi-component structures of CH_4 evolution rates of SH_14.7 coals in CO_2 the atmosphere are shown in Fig. 12 (the similar results of other particle sizes are not shown here). The fitting results almost perfectly match the experimental data, where the correlation coefficients of the lines are all greater than 0.999.

The proportions of the constituent reaction complexes of CH_4 evolution in the CO_2 atmosphere are summarized in Table 3. For better comparison, the characteristics of individual components of CH_4 evolution in the N_2 atmosphere are also listed there. In CO_2 environment, the amounts of the reaction type I and III are lower than those in N_2. Both of these constituent reactions are related to the direct decomposition of the functionalities that generate the methane precursors of methyl groups. Particularly, the constituent peak III of methane evolved in the CO_2 atmosphere shows a tremendous decrease, compared with that in N_2. As

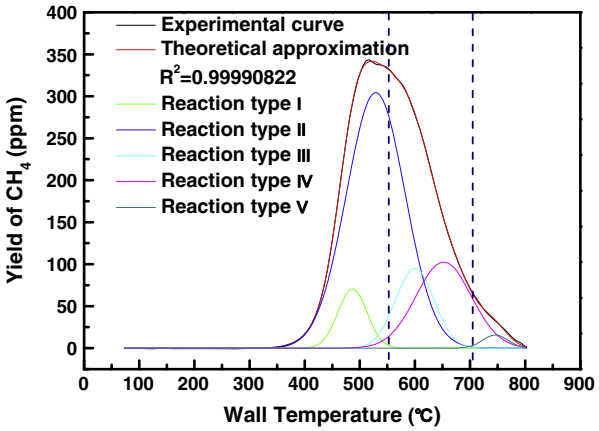

Fig. 12. Multi-component structure of CH_4 evolution rates during pyrolysis of SH_14.7 coals in the CO_2 atmosphere (heating rates 20 °C/min, temperature 800 °C, CO_2 atmosphere).

explained before, this is related to the higher density and heat capacity of CO_2. The bond cleavage reactions are limited because of the reduced heat delivered to the coal particles in CO_2 environment. The elimination rate of functional groups is delayed. Therefore, the dissociation of aryl methyl groups with high bonding energy are depressed, which leads to the decrease of the methane precursors and the subsequent methane yields. In addition, the other pyrolysis products like CO and H_2O during this stage compete for the donatable hydrogen for stabilization, which also reduces the evolution of CH_4. On the other hand, the methane formation involving the degradation of long chain groups all shows an increasing trend, i.e., the complex II of alkyl functionalities and peak IV of methylene/methine groups. Especially, the secondary pyrolysis related reaction type IV in the CO_2 atmosphere shows a significant increase compared with that in N_2. More large molecular systems are preserved in the coal pore structures because of the lower thermal and mass diffusivity of CO_2. The secondary pyrolysis reactions are more vigorous when certain temperature reaches and the pore structures are cracked. Thus, more methane is released. Furthermore, there are also slight differences of the peak V that the amounts of constituent reaction V in CO_2 are less than those in the N_2 atmosphere. The aromatic heterocyclic structures might be ruptured and depleted during the CO_2 gasification process of the nascent chars.

3.3. Influence of heating rate on the CH_4 formation mechanisms

The coal samples were heated up to 600 °C at 10, 20, 30, and 35 °C/min in N_2 and CO_2 atmospheres. The influence of different heating rates on the methane formation mechanism was investigated, and the typical evolution curves of SH_14.7 and SH_44.2 are shown in Fig. 13. With increasing the heating rates, the overall methane evolution curve shifts to a higher temperature, i.e. the temperature of the maximum methane-releasing rate is delayed. This phenomenon is associated with the heat and mass transfer limitations. The thermal lag phenomenon occurs during rapid surface heating [33,34]. The samples can be heated uniformly at lower heating rates. The temperature difference inside the coal particles is enlarged by increasing the heating rates, and a large thermal gradient is formed. Therefore, a greater fraction of methane precursors will be expended at higher temperatures.

Furthermore, with the increase of the heating rates, the evolution rates and total yields of methane increase tremendously. Intraparticle secondary reactions are responsible for more methane generation at higher heating rates. Tar cracking, rather than tar polymerization, is the dominant secondary reaction at high heating rates [34]. Higher heating rates provide less time for the generation, transport and reactions of large molecular systems in lower temperature ranges. Therefore, more functionalities are preserved to be released as methane precursors at higher temperatures. Larger heating rates increase the intraparticle concentration gradients, accelerating the internal mass transfer, which is advantageous for the methane evolution. Additionally, volatiles generated deep in the coal particle will experience an elevated temperature zone before escaping to the outside [34]. As a result, this increases the opportunity for intraparticle secondary reactions, promoting the methane formation.

On the other hand, with the increase of heating rates, the linewidths of methane–evolution curves turn out to be narrower. The coal particles are heated uniformly from the inside to the outside at lower heating rates. Lower heating rates provide more time for reactions to occur, and the dissociation of methane precursors is more adequate. Therefore, the constituent reactions are complete, and the gas releasing processes are prolonged at lower heating rates, which makes the overall methane evolution curve expand over a wider temperature range. With the heating rates increasing,

Table 3
Influence of pyrolysis atmospheres on the individual reaction complex of CH_4 evolution (heating rates 20 °C/min, temperature 800 °C, N_2 and CO_2 atmospheres).

Samples	N_2 peak I (%)	CO_2 peak I (%)	N_2 peak II (%)	CO_2 peak II (%)	N_2 peak III (%)	CO_2 peak III (%)	N_2 peak IV (%)	CO_2 peak IV (%)	N_2 peak V (%)	CO_2 peak V (%)
SH_14.7	6485	4657	40,201	40,553	12,023	8320	2656	12,855	757	899
SH_17.4	4891	4802	40,977	43,067	10,675	6912	6551	7426	1466	773
SH_21.3	5634	4080	20,429	43,220	21,348	9269	7569	9660	2415	1828
SH_44.2	7151	3566	35,047	37,376	18,480	13,094	3602	9766	1054	663

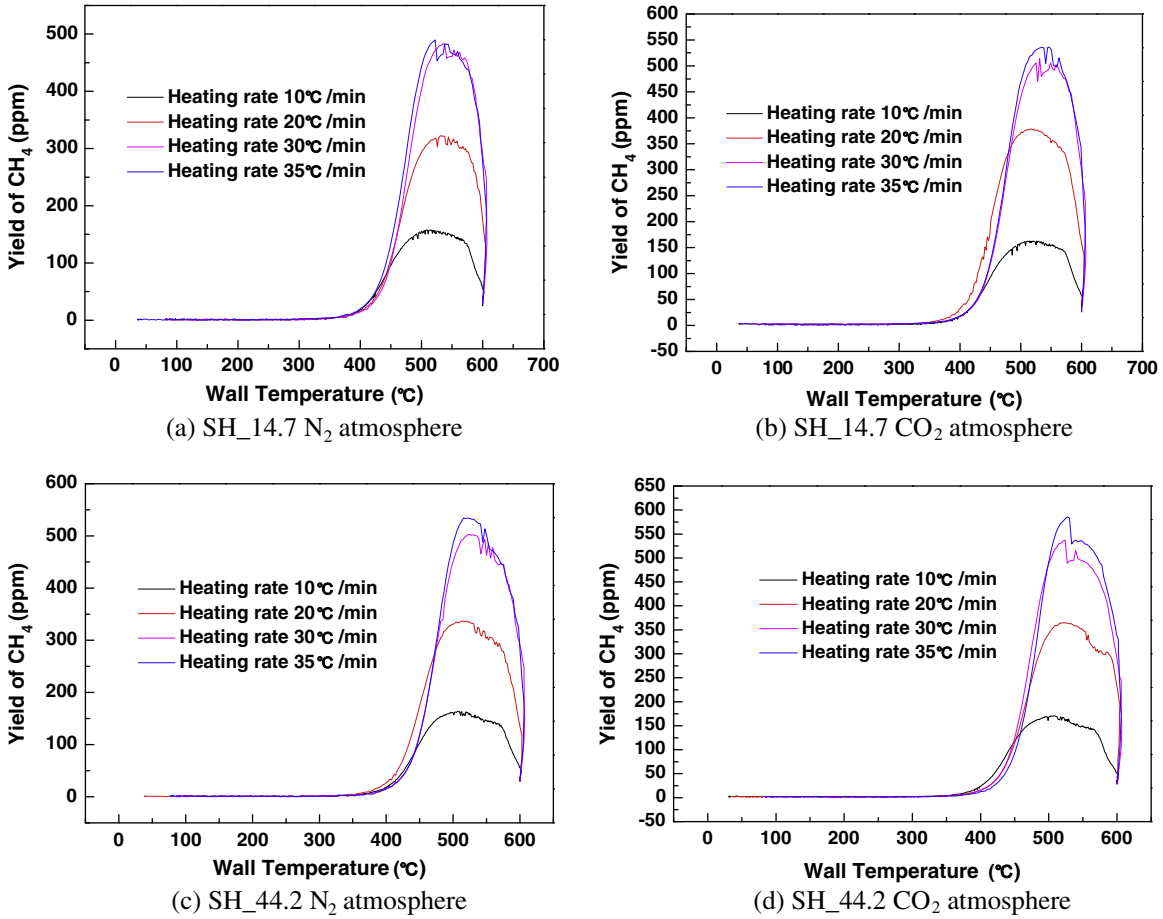

(a) SH_14.7 N_2 atmosphere (b) SH_14.7 CO_2 atmosphere

(c) SH_44.2 N_2 atmosphere (d) SH_44.2 CO_2 atmosphere

Fig. 13. Influence of heating rates on the evolution of CH_4 (heating rates 10, 20, 30, and 35 °C/min, temperature 600 °C, N_2 and CO_2 atmospheres).

the thermal gradient within the coal particles is enlarged, which provides less time for volatiles generation and decomposition reactions of functionalities during heatup. Competitive intraparticle processes for the consumption of methane precursors are more intense, which makes the constituent reactions more overlapped. Therefore, the gas-releasing processes are more concentrated, and the overall methane evolution curves are getting narrower at higher heating rates.

The kinetic studies were carried out under non-isothermal conditions in the work to better understand the CH_4 releasing process. The maximum temperatures of methane evolution rates were recorded at several different heating rates. The single first order model [4,13,18] can be applied to derive the kinetic parameters of CH_4 evolutions during coal pyrolysis. The pyrolytic reactions through the decomposition of functional groups are assumed to be first order reactions. The rate of individual CH_4 evolution can be described as:

$$\frac{dx}{dt} = -kx \tag{6}$$

where x represents the concentration of the unreleased substance that can be calculated by subtracting the amount already evolved from the ultimate yield of the species. The parameter k refers to the rate constant that often introduces the Arrhenius expression:

$$k = k_0 \exp\left(\frac{-E}{RT}\right) \tag{7}$$

where k_0 is the frequency factor or pre-exponential factor in s^{-1}; E represents the activation energy in (J mol^{-1}); R refers to the gas constant in (J mol^{-1} K^{-1}); T is the absolute temperature in K.

The coal samples were heated at a constant heating rate in non-isothermal experiments, which can be shown as:

$$\beta = \frac{dT}{dt} = \text{constant} \tag{8}$$

The temperature derivative of the evolution rate should be zero at the maximum evolution temperature T_{max}, which is shown in Eq. (9).

$$\frac{d(dx/dt)}{dT} = -x\frac{dk}{dT} - k\frac{dx}{dT} = 0 \tag{9}$$

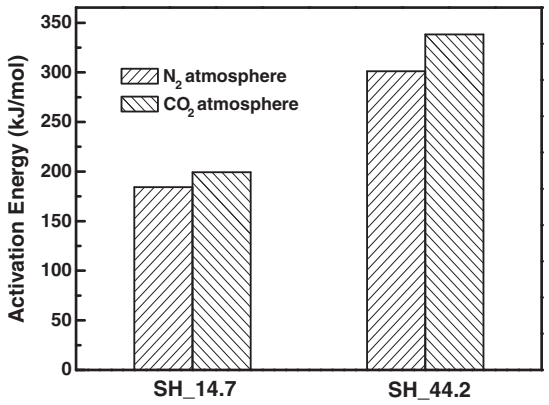

Fig. 14. Activation energies of CH_4 evolution during coal pyrolysis of SH_14.7 and SH_44.2 (heating rates 10, 20, 30, and 35 °C/min, temperature 600 °C, N_2 and CO_2 atmospheres).

Then, the kinetic parameters can be determined by substituting Eqs. (7) and (8) into Eq. (9):

$$-kx\left[\frac{E}{RT_{\max}^2}-\frac{k_0}{\beta}\exp\left(\frac{-E}{RT_{\max}}\right)\right]=0 \tag{10}$$

The logarithmic transformation of Eq. (10) results in a linear relationship between $\ln\left(\frac{\beta}{T_{\max}^2}\right)$ and $1/T_{\max}$. The activation energy E and the pre-exponential factor k_0 can be calculated through the slope and the intercept of the line [13].

$$\ln\left(\frac{\beta}{T_{\max}^2}\right)=-\frac{E}{RT_{\max}}+\ln\left(\frac{k_0R}{E}\right) \tag{11}$$

The activation energy influences the reaction rate significantly. The smaller the E is, the reaction rate is higher and the reactivity is better. Thus the release of the species becomes easier and more prompt. The activation energy of CH_4 evolution during coal pyrolysis determined by Eq. (11) is indicated in Fig. 14. The methane activation energies show a notable increase for larger coal particles in both N_2 and CO_2 atmospheres. The high values of E indicate that the release of methane is hard for large coal fractions, and the process is retarded. This is also in agreement with the observation from Fig. 3 that the maximum evolution temperatures are lower for superfine pulverized coal. Similarly, the lower thermal diffusivity and higher emissivity of CO_2 suppress the decomposition of methane precursors and the subsequent methane evolution, leading to the higher values of methane activation energies in the CO_2 atmosphere.

4. Conclusions

The mechanisms of methane formation during superfine pulverized coal pyrolysis in N_2 and CO_2 atmospheres are investigated under non-isothermal conditions in a fixed-bed reactor. The following conclusions can be drawn:

1. The CH_4 formation curve during coal pyrolysis shows a broad single peak, which is attributed to several constituent reactions leading to the multi-component structure. The peak temperatures of CH_4 evolution rates shift towards higher temperature ranges with the increase of coal ranks.
2. There is a critical particle size for the maximum release of CH_4. The CH_4 evolution rate for SH_21.3 coal is largest, while NMG coals with particle sizes of 12.5 μm release CH_4 fastest. The lower ranking coals with relatively small particle sizes have stronger reduction effects of light hydrocarbons.
3. Three main stages of CH_4 evolution during coal pyrolysis are visible, which are in the range of 300–550 °C, 550–700 °C and over 700 °C, separately. The total overlapped CH_4 evolution curves are resolved applying the deconvolution method through numerical analysis. In our experimental ranges, five constituent reaction complexes induced by different functional groups are recognized to comprise the overall CH_4 evolution curves during coal pyrolysis.
4. Five CH_4 precursors involving in the evolution process during coal pyrolysis are confirmed, combining the solid-state ^{13}C NMR analysis. The reaction type I is related to the methoxy groups in coal, while the cleavage of alkyl side chains results in the evolution of type II methane. Strongly bonded aryl methyl groups are recognized as the methane precursors of peak III. The constituent reaction complex IV initiated from secondary pyrolysis reactions is also an important source of CH_4. The cleavage of aromatic heterocyclic structures might be responsible for the release of the late type V CH_4. The reaction complex II is positively correlated to the overall maximum CH_4 evolution temperatures.
5. Replacing N_2 with CO_2 can enhance the CH_4 releasing rates, while the total yields of CH_4 are depressed. The constituent reaction complexes are more overlapped in the CO_2 atmosphere, causing the overall CH_4 evolution peak widths to be narrower. In the CO_2 environment, the amounts of the reaction type I and III are lower than those in N_2, while the complexes II and IV show the opposite trends. With the increase of the heating rates, the overall CH_4 evolution curve shifts to a higher temperature, and the evolution rates and total yields of methane increase tremendously. The CH_4 releasing processes are more concentrated and overlapped. The overall methane evolution curves are narrowing at higher heating rates.

Acknowledgements

This work was supported by the National Natural Science Foundation of China (Grant Nos. 51306116 and 51376131). The authors are grateful to the Instrumental Analysis Center of SJTU for giving the opportunity for the TGA experiments.

References

[1] Shabbar S, Janajreh I. Thermodynamic equilibrium analysis of coal gasification using Gibbs energy minimization method. Energy Convers Manage 2013;65:755–63.
[2] Solomon PR, Serio MA, Suuberg EM. Coal pyrolysis: experiments, kinetic rates and mechanisms. Prog Energy Combust Sci 1992;18:133–220.
[3] Ofosu-Asante K, Stock LM, Zabransky RF. Preparation and pyrolysis of O-(Alkylphenyl)methyl and O-(Alkylnaphthyl)methyl Illinois No. 6 coals. Role of dealkylation reactions in gaseous hydrocarbon formation. Energy Fuel 1988;2:511–22.
[4] Serio MA, Hamblen DG, Markham JR, Solomon PR. Kinetics of volatile product evolution in coal pyrolysis: experiment and theory. Energy Fuels 1987;1:138–52.
[5] Zhang CQ, Jiang XM, Wei LH, Wang H. Research on pyrolysis characteristics and kinetics of super fine and conventional pulverized coal. Energy Convers Manage 2007;48:797–802.
[6] Liu JX, Jiang XM, Han XX, Shen J, Zhang H. Chemical properties of superfine pulverized coals. Part 2. Demineralization effects on free radical characteristics. Fuel 2014;115:685–96.
[7] Shen J, Liu JX, Zhang H, Jiang XM. NOx emission characteristics of superfine pulverized anthracite coal in air-staged combustion. Energy Convers Manage 2013;74:454–61.
[8] Liu JX, Gao S, Jiang XM, Shen J, Zhang H. NO emission characteristics of superfine pulverized coal combustion in the O_2/CO_2 atmosphere. Energy Convers Manage 2014;77:349–55.
[9] Liu JX, Jiang XM, Huang XY, Shen J, Wu SH. Investigation of the diffuse interfacial layer of superfine pulverized coal and char particles. Energy Fuels 2011;25:684–93.
[10] Liu JX, Jiang XM, Huang XY, Wu SH. Morphological characterization of super fine pulverized coal particle. Part 2. AFM investigation of single coal particle. Fuel 2010;89:3884–91.

[11] Porada S. The reactions of formation of selected gas products during coal pyrolysis. Fuel 2004;83:1191–6.
[12] Burnham AK, Braun RL. Global kinetic analysis of complex materials. Energy Fuels 1999;13:1–22.
[13] Holstein A, Bassilakis R, Wójtowicz MA, Serio MA. Kinetics of methane and tar evolution during coal pyrolysis. Proc Combust Inst 2005;30:2177–85.
[14] Arenillas A, Rubiera F, Pis JJ. Simultaneous thermogravimetric-mass spectrometric study on the pyrolysis behavior of different rank coals. J Anal Appl Pyrol 1999;50:31–46.
[15] Arenillas A, Rubiera F, Pis JJ, Cuesta MJ, Iglesias MJ, Jiménez A, et al. Thermal behaviour during the pyrolysis of low rank perhydrous coals. J Anal Appl Pyrol 2003;68–69:371–85.
[16] Cramer B. Methane generation from coal during open system pyrolysis investigated by isotope specific, Gaussian distributed reaction kinetics. Org Geochem 2004;35:379–92.
[17] Jüntgen H, van Heek KH. An update of German non-isothermal coal pyrolysis work. Fuel Process Technol 1979;2:261–93.
[18] Jüntgen H. Review of the kinetics of pyrolysis and hydropyrolysis in relation to the chemical constitution of coal. Fuel 1964;63:731–7.
[19] Kelemen SR, Kwiatek PJ. Quantification of organic oxygen species on the surface of fresh and reacted Argonne premium coal. Energy Fuels 1996;9:841–8.
[20] Hodek W, Kirschstein J, van Heek KH. Reactions of oxygen containing structures in coal pyrolysis. Fuel 1991;70:424–8.
[21] Kok MV. Simultaneous thermogravimetry–calorimetry study on the combustion of coal samples: effect of heating rate. Energy Convers Manage 2012;53:40–4.
[22] van Heek KH, Hodek W. Structure and pyrolysis behaviour of different coals and relevant model substances. Fuel 1994;73:886–96.
[23] Charpenay S, Serio MA, Bassilakis R, Solomon PR. Influence of maturation on the pyrolysis products from coals and kerogens. 1. Experiment. Energy Fuels 1996;10:19–25.
[24] Cramer B, Faber E, Gerling P, Krooss BM. Reaction kinetics of stable carbon isotopes in natural gas- insights from dry, open system pyrolysis experiments. Energy Fuels 2001;15:517–32.
[25] Kelemen SR, Afeworki M, Gorbaty ML, Cohen AD. Characterization of organically bound oxygen forms in lignites, peats, and pyrolyzed peats by X-ray photoelectron spectroscopy (XPS) and solid-state ^{13}C NMR methods. Energy Fuels 2002;16:1450–62.
[26] Solomon PR, Hamblen DG, Serio MA, Yu ZZ, Charpenay S. A characterization method and model for predicting coal conversion behavior. Fuel 1993;72:469–88.
[27] Gorbaty ML, Maa PS. A critical temperature threshold for coal hydropyrolysis. Fuel Process Technol 1987;15:91–100.
[28] Karcz A, Porada S. Formation of C1–C3 hydrocarbons during pressure pyrolysis and hydrogasification in relation to structural changes in coal. Fuel 1995;74:806–9.
[29] Saptoro A, Huo KC. Influences of Indonesian coals on the performance of a coalfired power plant with an integrated post combustion CO_2 removal system: a comparative simulation study. Energy Convers Manage 2013;68:235–43.
[30] Duan L, Zhao CS, Zhou W, Qu CR, Chen XP. Investigation on coal pyrolysis in CO_2 atmosphere. Energy Fuels 2009;23:3826–30.
[31] Buhre BJP, Elliott LK, Sheng CD, Gupta RP, Wall TF. Oxy-fuel combustion technology for coal-fired power generation. Prog Energy Combust 2005;31:283–307.
[32] Molina A, Shaddix C. Ignition and devolatilization of pulverized bituminous coal particles during oxygen/carbon dioxide coal combustion. Proc Combust Inst 2007;31:1905–12.
[33] Yang HP, Yan R, Chin T, Liang DT, Chen HP, Zheng CG. Thermogravimetric analysis-fourier transform infrared analysis of palm oil waste pyrolysis. Energy Fuels 2004;18:1814–21.
[34] Griffin TP, Howard JB, Peters WA. An experimental and modeling study of heating rate and particle size effects in bituminous coal pyrolysis. Energy Fuels 1993;7:291–305.